



Strength and deformation of RC column retrofitted using aramid belts with large spacing

N. Hanai,¹ T. Ichinose,² K. Kosugi,³ and M. Takeda⁴

ABSTRACT

A new method is proposed to strengthen reinforced concrete columns connected to walls. First, holes are drilled through the walls with an interval less than a half of the column depth. Second, aramid sheet is pasted on the column. Third, aramid belts are bound around the column. Five series of experiments are conducted to investigate (1) shear strength, (2) bond-splitting strength, (3) ductility under low axial force, and (4) ductility under high axial force. A set of design equations are proposed to predict the capacity of the columns retrofitted using the proposed procedure.

Introduction

Aramid is a long-chain synthetic polymer with amide linkages (-CO-NH-). The aramid we use has tensile strength of approximately 3,000 MPa (much stronger than steel) and Young's modulus of 150 GPa (less stiff than steel). In Japan, aramid fiber is becoming popular as a material for jacketing reinforced concrete columns to increase their shear strengths. The advantage of aramid fiber over steel plate and carbon fiber is its flexibility that makes retrofitting work easier.

Many experiments have been done to investigate the effects of aramid fiber to jacket RC columns (AIJ 2002). However, such jacketing cannot be applied to columns connected to walls or beams connected to slabs. The objective of this paper is to develop a reliable method to retrofit such columns and beams.

Procedure of retrofit and experiment plan

We propose the following procedure:

- (a) Drill holes through the walls with an interval less than a half of the column depth (Fig. 1a).
- (b) Paste aramid-sheet on the column using epoxy adhesive (Fig. 1b).
- (c) Bind aramid-belts around the column using epoxy adhesive (Fig. 1c).

We assume that the retrofit is needed for the shear force indicated by an arrow in Fig. 1c. We neglect the contribution of the wing walls parallel to the shear force because their failure mode

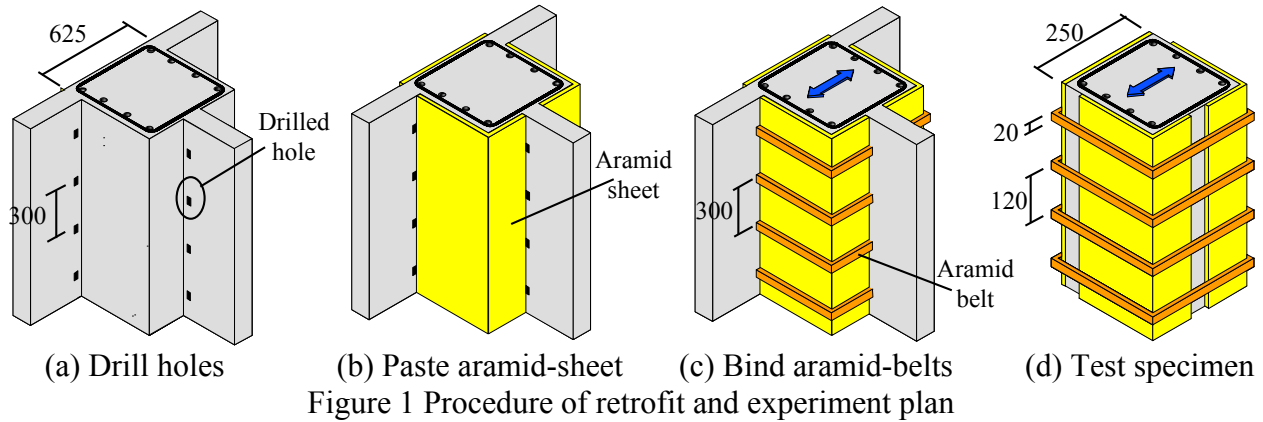
¹Assistant Professor, Dept. of Architecture, Kyushu Sangyo University, Fukuoka, Japan

² Professor, Dept. of Architecture, Nagoya Institute of Technology, Nagoya, Japan

³ Engineer, Fibex Corporation, Tokyo, Japan

⁴ Associate Professor, Dept. of Civil Engineering, Tohoku Gakuin University, Sendai, Japan

shall be brittle. The contribution of the wall perpendicular to the shear force shall also be negligible. Therefore, we conduct experiments using the test specimens shown in Fig. 1d.



Shear strength

Six specimens listed in Table 1 were tested to investigate the shear strength. High strength steel ($f_y = 915$ MPa) was used as longitudinal reinforcement to prevent flexural failure. The diameter of hoop was 4 mm and the spacing was 120 mm. Specimen S1 had no strengthening. Specimen S2 had uniformly wrapped aramid-sheet (Fig. 2a) 0.43 mm thick. The shear reinforcement ratio (the thickness divided by the width of the column) was 0.34%. Specimen S3 had aramid belts of the same thickness and 20 mm wide (Fig. 2b). To make the shear reinforcement ratio equivalent to that of S2, we tied the belt six times at the interval of 120 mm (or clear spacing of 100 mm). Specimens S4-S6 had same amount of aramid belts as well as aramid sheet 0.076 mm thick (Fig. 2c). The direction of the fiber of the sheet was horizontal for S4 and S6, whereas that for S5 was vertical.

The axial load was kept constant at 20 % of the axial capacity (250 kN for S1-S5 and 304 kN for S6). The horizontal load was applied monotonically for S1-S5 as shown in Fig. 3a. Test results are shown in Fig. 3b. The strength of Specimen S3 with belts only was smaller than that of Specimen S2 with uniform sheet. Specimen S4 with belts and sheet of the horizontal direction had the largest strength, though the sheet broke along the edges of the belts as shown in Fig. 2c at large deflection. Specimen S6 was loaded keeping contra-flexure point at mid-span (Fig. 4a). The concrete expanded between the belts as shown in Fig. 4b. Figure 4c shows the observed load-deformation relationship.

Table 1 List of specimens (shear strength series)

Name	Shear span ratio	Conc. strength	Aramid sheet	Aramid belt	Observed strength
S1	1.6	15.6 MPa	None		93 kN
S2			$t = 0.43$ mm, uniform		186 kN
S3			None	$t = 0.43$ mm x 6 $w = 20$ mm $s = 100$ mm	165 kN
S4			$t = 0.076$ mm		221 kN
S5					171 kN
S6					257 kN
	0.72	24.3 MPa			



(a) S2 (uniformly wrapped)

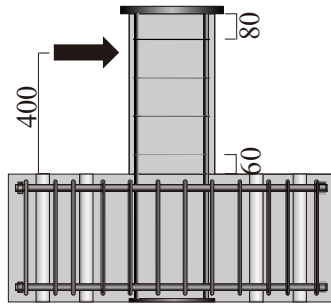


(b) S3 (belt only)

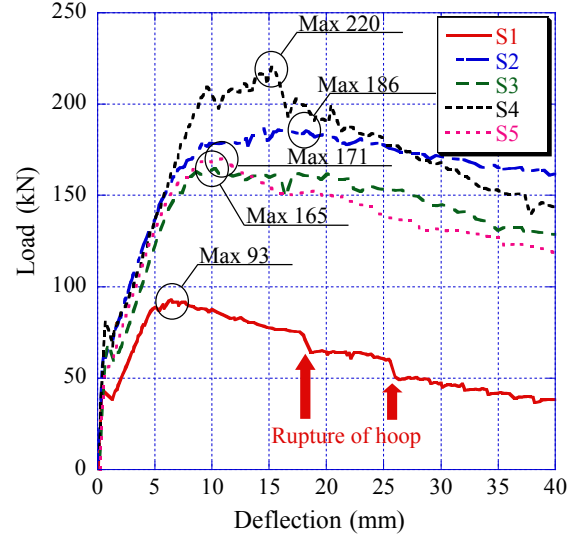


(c) S4 (belt and sheet)

Figure 2 Photos taken after the tests

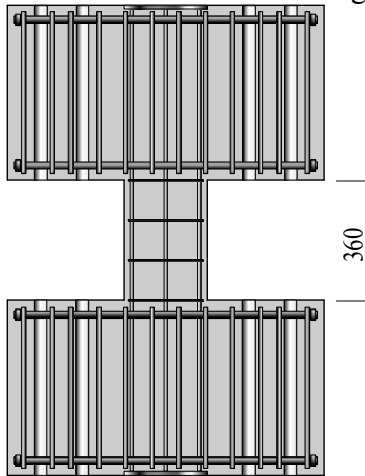


(a) Specimen



(b) Load-deformation relationship

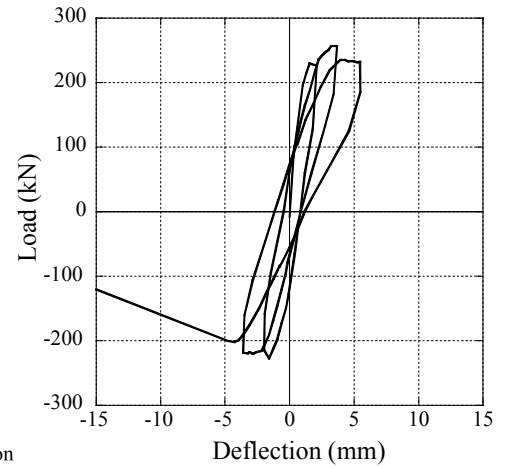
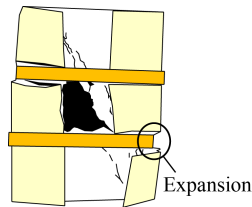
Figure 3 Specimens with shear span ratio of 1.6



(a) Specimen S6



(b) Expansion of concrete



(c) Load-deformation relation

Figure 4 Specimen S6 with shear span ratio of 0.72

We measured the deformation of the belts as shown in Fig. 5a. The results of Specimen S4 are shown in Fig. 5b, where the blue line indicates the deformation at the deflection of 10 mm (before the strength) and the green line indicates the deformation at the deflection of 18 mm (after the strength). This indicates that the shear failure occurred in the zone shown in Fig. 5c, because the strain at the center of the section was larger than 0.03 (Fig. 6a) whereas that at the surface of the belt was less than 0.008 (Fig. 6c).

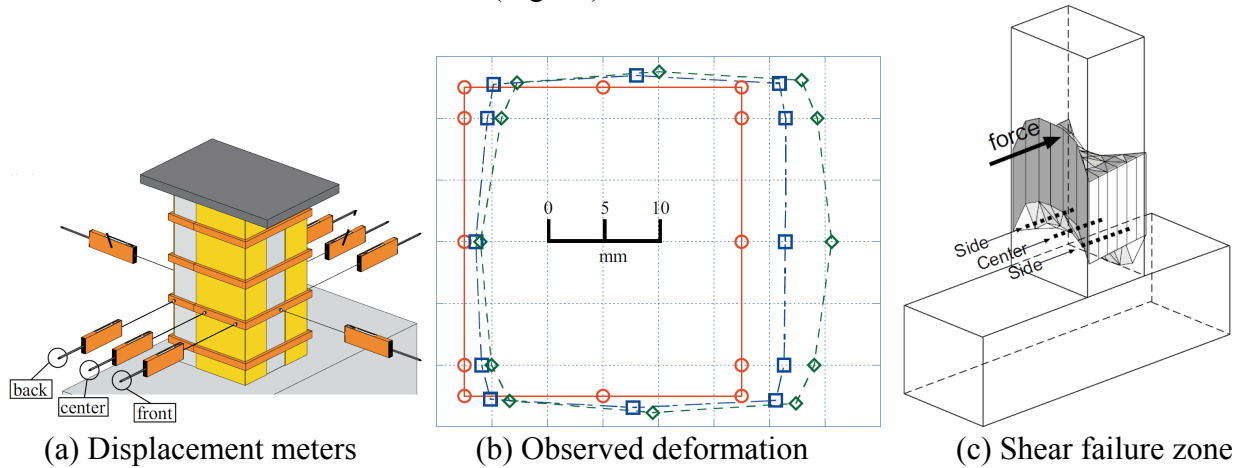


Figure 5 Deformation of Specimen S4

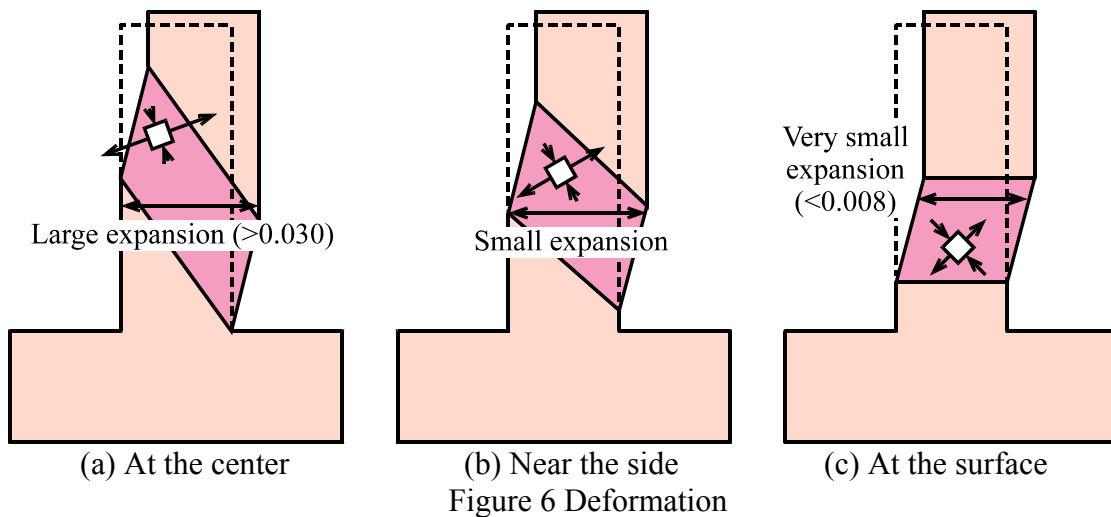
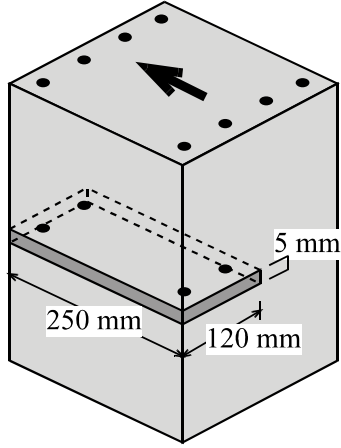
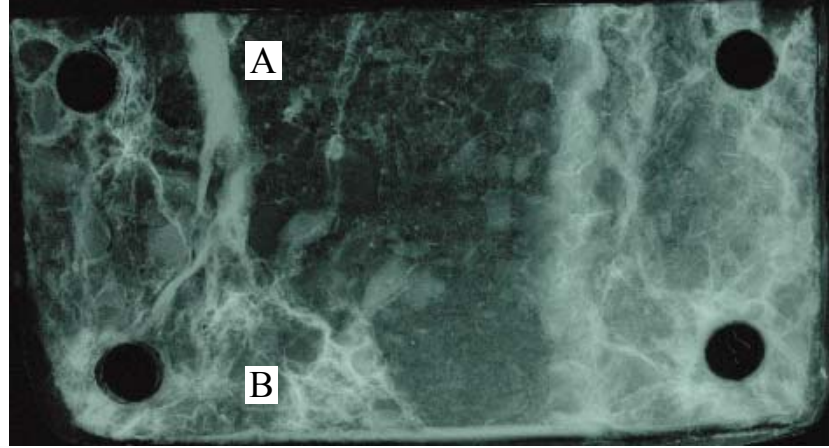


Figure 6 Deformation

In order to investigate the cracks inside the retrofitted columns, another specimen was constructed and loaded similarly. When the maximum deflection was attained, contrast agent mixed with epoxy resin was injected into the cracks of the specimen. The specimen was then unloaded and thawed into as shown in Fig. 7a. Then, we took X-ray photographs of the cracks inside the specimen. The black circles in Fig. 7b are the longitudinal reinforcement made of carbon rod (we did not use steel bars because they absorb X-ray too much). The bold white line A is a wide shear crack at the center of the section indicating tensile shear failure. The crack A branches into numerous fine cracks (cracks B) near the aramid belts indicating compressive shear failure.



(a) Thawed section



(b) X-ray photograph

Figure 7 Cracks inside the specimen

Japanese engineers use the following equation to predict shear strength (JBDPA 2001).

$$V_u = 0.8 \times (\tau_c + \tau_s + 0.1\sigma_0) bD \quad (1)$$

where

b : width of section

D : depth of section

$$\tau_c = \frac{0.053 p_t^{0.23} (17.6 + f'_c)}{M/(Vd) + 0.12} \quad (\text{contribution of concrete}) \quad (2)$$

p_t : tensile reinforcement ratio

f'_c : concrete strength

$M/(Vd)$: shear span ratio

$$\tau_s = 0.845 \sqrt{p_w f_{wy}} \quad (\text{contribution of shear reinforcement}) \quad (3)$$

p_w : shear reinforcement ratio

f_{wy} : yield stress of shear reinforcement

$$\sigma_0 = \frac{P}{bD} \quad (\text{average stress caused by axial force, } P) \quad (4)$$

For columns retrofitted with aramid fiber, we need to consider the fact that the strain in aramid fiber seldom exceeds 0.008. We also need to consider the detrimental effect of spacing of aramid belt and the advantage of aramid sheet pasted under belts. Therefore, we propose to modify the second term as follows.

$$\tau_s = 0.845 \sqrt{p_w f_{wy} + \left(1 - \frac{s}{\alpha D}\right) p_f f_{fd}} \quad (5)$$

where

s : clear spacing of aramid belt (e.g. $s = 120 - 20 = 100$ mm for Fig. 1d)

p_f : shear reinforcement ratio of aramid belt, $p_f = (\text{width}) \times (\text{thickness}) / (\text{interval})$

f_{fd} : effective strength of aramid fiber

($f_{fd} = 0.008 E_{fd}$ where E_{fd} is Young's modulus of aramid fiber)

α : sheet factor

($\alpha = 3$ if aramid sheet is pasted under belts in the horizontal direction, and $\alpha = 1$ if not).

Figure 8 compares the observed and calculated strengths, including specimens AT00-15 (uniform sheet of $t = 0.29$ mm) and AT10-15 ($t = 0.29$ mm, $w = s = 38$ mm) tested by Kosato et al (1999). The observed strengths agree conservatively with the calculated ones.

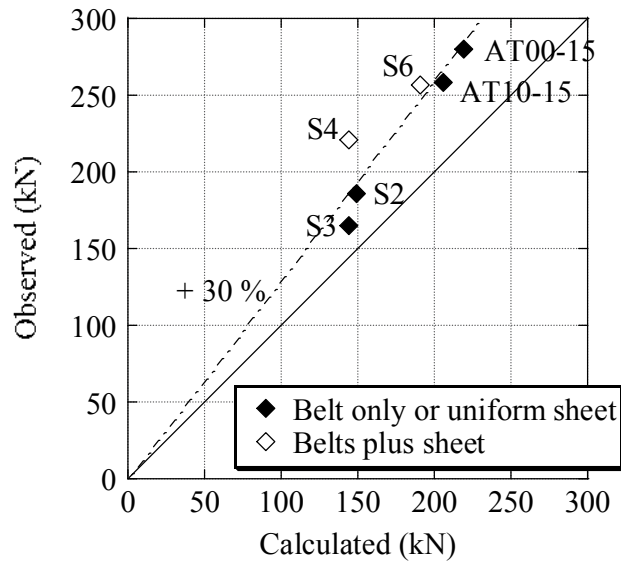


Figure 8 Observed and calculated strengths

Deformation capacity under low axial load

Cyclic loading tests were conducted under axial load of 250 kN (20 % of the axial capacity). The concrete strength was 19.9 MPa. The yield strength of the longitudinal reinforcement was 360 MPa. The other parameters were similar to those of Specimens S1-S5. Figure 10 shows the test results, where the arrows and the circles indicate the load steps at the strengths and those at 80% of the strengths, respectively. Specimen L5 with belts and sheet (Fig. 9d) attained the calculated flexural strength (154 kN) and large deformation capacity ($R = 18/400 = 0.045$ rad), though we note the detrimental effect of large spacing if compared with Specimen L2.

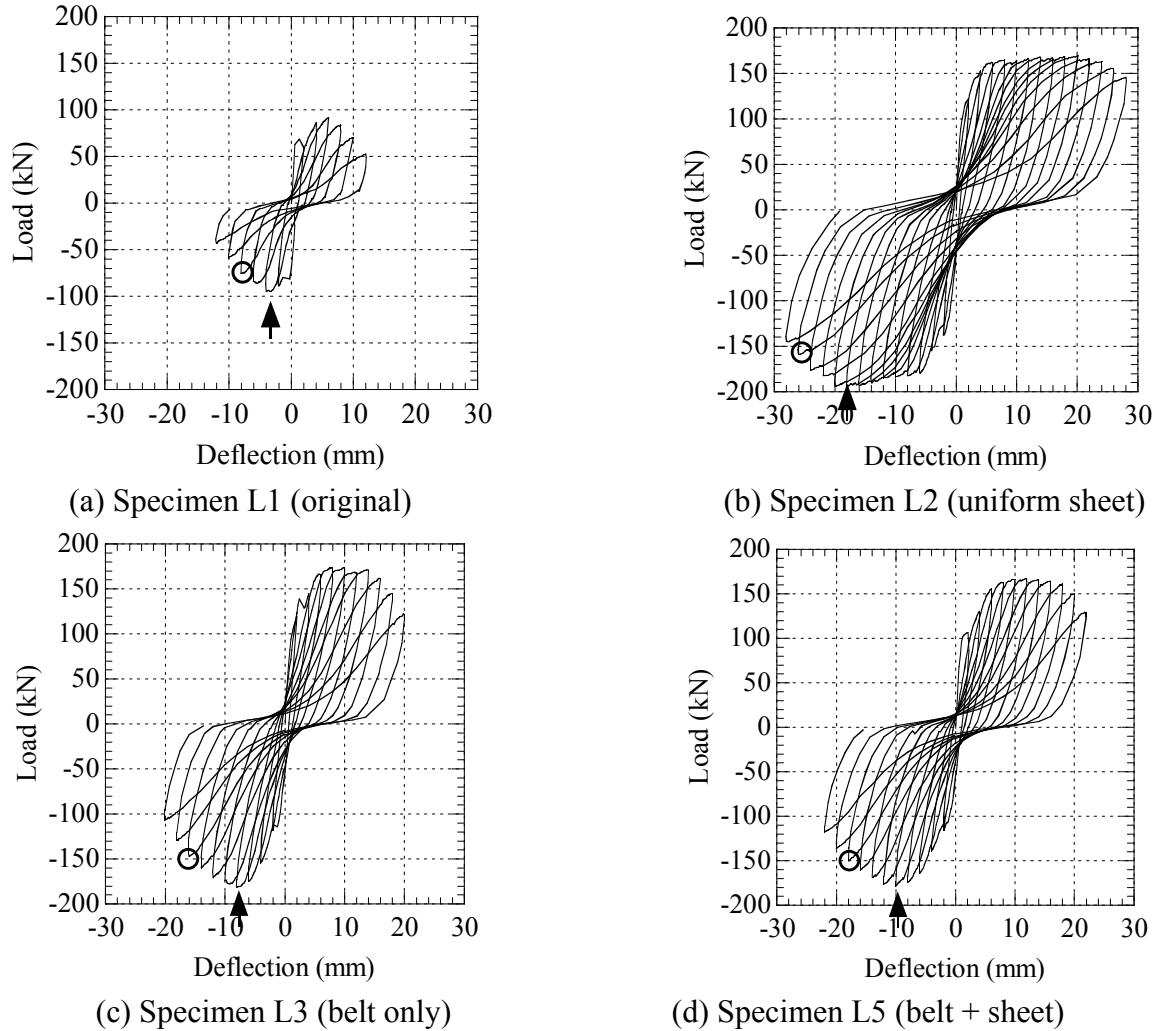


Figure 9 Test results of low-axial-load series

Deformation capacity under high axial load

Cyclic loading tests were conducted under axial load of 500 kN (33 % of the axial capacity). The concrete strength was 24.3 MPa. The yield strength of the longitudinal reinforcement was 381 MPa. The other parameters were similar to those of Specimens S1-S5. Figure 10 shows the test results. Specimen H3 with belts and sheet (Fig. 10c) attained the calculated flexural strength (202 kN) and deformation capacity of $R = 10/400 = 0.025$ rad. Specimen H2 with uniform sheet showed larger ductility but its strength was smaller than that of Specimen H3.

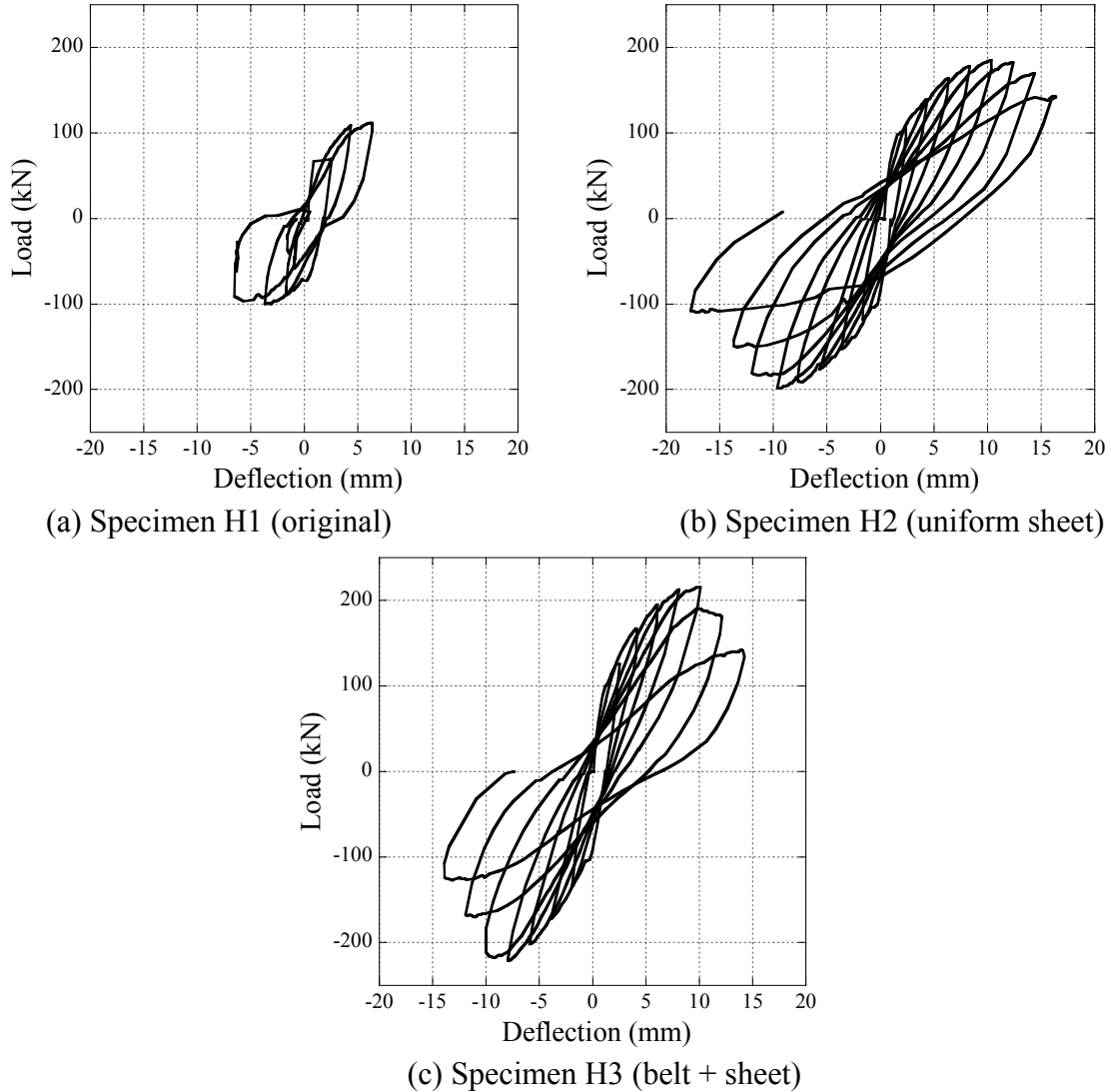


Figure 10 Test results of high-axial-load series

Bond splitting failure

Figures 11a-b show the test specimens to investigate the bond splitting failure. The concrete strength was 24.3 MPa. The yield strength of the longitudinal reinforcement was 855 MPa to ensure the bond splitting failure. Figures 11c-e show the specimens after testing and removing the sheet. Bond cracks were observed in all the specimens.

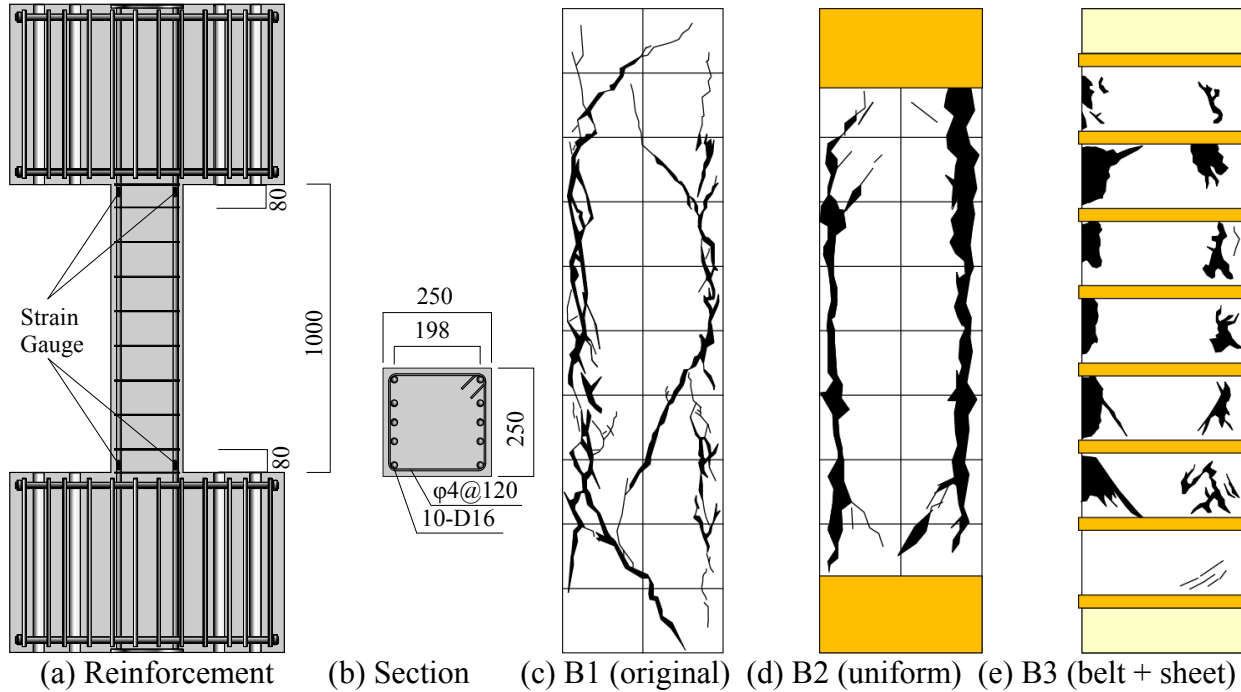


Figure 11 Test specimens of bond failure series

Cyclic loading tests were conducted under axial load of 20 % of the axial capacity. Figure 12 shows the observed load-deflection relationships. The deformation capacity of Specimen B3 with belts and sheet (Fig. 12c) was comparable with that of Specimen B2 with uniform sheet and much larger than Specimen B1 without retrofit (Fig. 12a). According to the strain gages attached at the critical sections (Fig. 11a), the bond stress was the largest at the strength (the arrows in Fig. 12) and decreased to 1/3 or 1/4 of the maximum stress at the largest deflection. We conclude that the retrofit did not prevent the bond failure but prevented premature failure. The observed strengths of Specimens B2 and B3 (179 and 178 kN) conservatively agreed with those calculated using Equations 1, 2, 4 and 5 (159 and 157 kN).

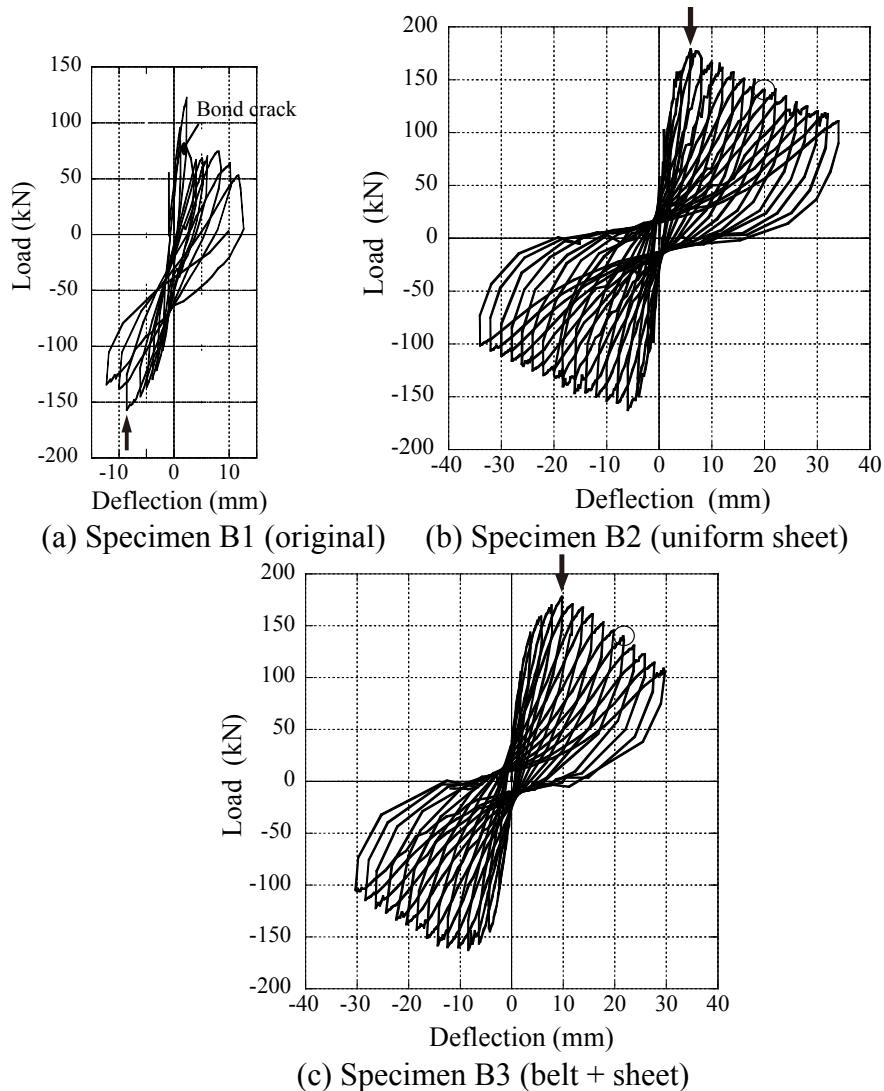


Figure 12 Observed load-deflection relationships

Conclusions

The retrofit shown in Figure 1 enhanced strength and/or ductility of RC column, irrespective of its failure mode (shear, flexure or bond), shear span ratio, and the amount of axial force. The enhancement was similar to that obtained by uniform aramid sheet. The observed strengths of the specimens that failed in shear or bond conservatively agreed with those calculated using Equations 1, 2, 4 and 5.

References

- Architectural Institute of Japan, 2002. *Guidelines for seismic retrofit of concrete structures using continuous fiber*, 505 pages (in Japanese)
- Japan Building Disaster Prevention Association, 2001. *Standard for seismic evaluation and retrofit*, 283 pages. (in Japanese)
- T. Kosato, M. Nagasaka, and S. Shimoda, 1999. Effects of aramid fiber on ductility of existing RC columns, *Proc. of AIJ annual conference*, pp. 85-86 (in Japanese)